ELSEVIER

S0032-3861(96)00524-1

Polymer Vol. 38 No. 2, pp. 255–261, 1997

0032-3861/97/$17.00 + 0.00

Dielectric relaxation of the electric field in poly(vinyl acetate): a time domain study in the range 10^{-3}–10^{6} s

Hermann Wagner and Ranko Richert*

Max-Planck-Institut für Polymerforschung, Ackermannweg 10, 55128 Mainz, Germany

(Received 10 January 1996; revised 22 April 1996)

We have measured the polarization of poly(vinyl acetate) in terms of a real dielectric relaxation technique by studying the decay of the electric field $E(t)$ for times 10^{-3} s $\leq t \leq 10^{6}$ s under the condition of a constant dielectric displacement for $t > 0$. This represents a direct measurements of the dielectric modulus $M(t)$, opposed to the conventional method of measuring the dielectric retardation $\epsilon(t)$, or its frequency domain analogue $\epsilon^*(\omega)$. The advantages of accessing $M(t)$ are a simple experimental set-up and for polar materials experimental times which are shorter by at least a factor of $\epsilon_s/\epsilon_\infty$ relative to $\epsilon(t)$ decays. The latter effect is based on the well-known relation $\tau_L = \epsilon_\infty/\epsilon_s\tau_D$ between transversal and longitudinal dielectric time constants. For the polymer under study, we find that no significant change of the relaxation time distribution occurs within the experimental time window, i.e. from well above the glass transition at T_g (if defined via $\tau_g = \tau(T_g) = 100$ s) to temperatures below T_g where the average retardation times $\langle\tau\rangle$ attain values of up to 10^7 s. Copyright © 1996 Elsevier Science Ltd.

(Keywords: dielectric relaxation and retardation; glass transition; relaxation time distribution)

INTRODUCTION

The dynamics of polymers have been studied extensively by techniques which measure the dielectric relaxation involved in the motion of the macromolecule or subunits thereof[1]. Among the diversity of modes detectable by this method are various local motions of polar side-groups, segmental motion as well as normal modes. Usually, the structural relaxation or α-process is linked to segmental modes which dominate in determining the viscous behaviour and the glass transition at $T = T_g$. Due to the low or absent tendency to crystallize found for most polymeric materials, lowering the temperature can drastically increase the average time-scales of relaxation processes until at $T = T_g$ the system experiences a transition from the (supercooled) liquid to the glassy or disordered solid state[2]. Although no rigorous definition of T_g exists, it is common practice to employ calorimetric data or absolute values such as the temperature at which the viscosity η attains 10^{13} P or, alternatively, at which a specified average relaxation time $\langle\tau\rangle$ reaches a value of 100 s[3]. In the following, glass transition temperatures inferred from one of the above-mentioned three methods will be denoted T_g*, in order to differentiate T_g* from a T_g based on ergodicity arguments. A more kinetic approach relates T_g to the situation where the system becomes non-ergodic within a given time-scale of the experiment. Such an understanding of the glass transition implies that T_g shifts to lower temperatures as the experimental time is extended, which expresses the commonly accepted idea of the glass transition being a purely kinetic effect and T_g being affected by the particular experimental conditions[4,5], e.g. by the cooling rate in a differential scanning calorimetry experiment. It is clearly impossible to measure relaxation processes below T_g if defined in such a manner.

As a universal feature of polymers one commonly finds a variation of the average relaxation time $\langle\tau\rangle$ with temperature which is well represented by the Vogel–Fulcher–Tammann (VFT)[6,7] expression

$$\langle\tau\rangle = \langle\omega^{-1}\rangle = A\exp[B/(T - T_0)] \qquad (1)$$

or equivalently by the Williams–Landel–Ferry (WLF) law, where in equation (1) the parameters A, B, and T_0 are assumed to be independent of temperature. Similarly common is the appearance of a broad distribution of relaxation times as a signature of a significant deviation from exponential decay behaviour or from a susceptibility of the Debye type. In terms of a simple empirical function, such a dispersive decay $\phi(t)$ can often be accounted for using the stretched exponential or Kohlrausch–Williams–Watts (KWW)[8,9] function

$$\phi(t) = \phi_0\exp[-(t/\tau_{KWW})^{\beta_{KWW}}] \qquad (2)$$

In the KWW expression, τ_{KWW} is a characteristic relaxation time and β_{KWW} within the limits $0 < \beta_{KWW} < 1$ quantifies the extent of deviation from pure exponentiality or equivalently the degree of the relaxation time dispersion, whereas the case $\beta_{KWW} = 1$ refers to simple exponential behaviour. In cases where the distribution of relaxation times (or equivalently β_{KWW}) is temperature-invariant, the changes in T reduce to a rescaling of the time axis such that shifting the curves along the log(t) scale lets the data coincide on a single master curve. This time–temperature superposition

* To whom correspondence should be addressed

principle is not generally valid, but holds for a number of polymers in a limited temperature interval[10]. With respect to the nature of the glass transition it is of interest to what extent the shape of the distribution of relaxation times is maintained upon cooling to well below T_g*. Nozaki and Mashimo[11] have addressed this problem using a combination of frequency domain spectroscopy and time domain dielectric spectroscopy for poly(vinyl acetate) (PVAc), and conclude that an abrupt change in the retardation time spectrum occurs at $T = T_g$*, implying that other than purely kinetic effects occur around T_g.

Dielectric spectroscopy is an ideal method for investigating relaxation times and their dispersion over a large temperature range and with high precision. For intermediate time-scales a common technique is the frequency domain impedance or gain-phase analysis in the range $10^{-3}\,\text{Hz} \leq f \leq 10^{7}\,\text{Hz}$ applied to a capacitor filled with the dielectric material under study[12]. Longer time-scales are usually accessed by time domain techniques[1,13,14], where at $t = 0$ a voltage step is applied to the capacitor and the time-resolved polarization $P(t) \propto D(t) \propto \int I(\text{t})\text{dt}$ is obtained by recording the current $I(t)$[1] or displacement $D(t)$[13]. Common to these approaches is the experimental condition of the externally applied voltage (or field E_0) being independent of the progress of polarization, i.e. in the time domain case $P(t)$ is measured under the condition $\text{d}E/\text{d}t = 0$ for $t > 0$, such that the results refer directly to the dielectric function $\epsilon(t)$ or $\epsilon^*(\omega)$.

For the present investigation we follow an alternative route for measuring $P(t)$ in the time domain by applying at $t = 0$ a certain displacement D_0 and acquiring the time-dependent voltage or field $E(t)$ under the condition $\text{d}D/\text{d}t = 0$ for $t > 0$. In this case, we have $P(t) \propto E(t)$, and the results refer to the dielectric modulus $M(t)$. If transformed into the frequency domain equivalent $M^*(\omega)$, the relation to the dielectric function is simply given by $M^*(\omega) = 1/\epsilon^*(\omega)$[15]. Although the two quantities reflect the same microscopic effects, namely orientational polarization of permanent dipoles, their characteristic time-scales $\langle\tau\rangle$ as well as the corresponding distributions of τ can differ significantly. For the simple Debye case of a single relaxation time the relation between the constant field (τ_ϵ) and constant displacement (τ_M) time constants can be obtained from a straightforward calculation and reads $\tau_M = \tau_\epsilon \epsilon_\infty/\epsilon_s$[16], where ϵ_∞ and ϵ_s denote the dielectric constants in the limit of high and low frequencies, respectively. For most realistic, i.e. non-Debye, materials displaying a broad distribution of relaxation times, the relation between $\langle\tau_M\rangle$ and $\langle\tau_\epsilon\rangle$ has to be evaluated numerically with the result that the ratio $\langle\tau_M\rangle/\langle\tau_\epsilon\rangle$ attains values significantly below $\epsilon_\infty/\epsilon_s$[17,18]. The interesting consequence for dielectric experiments on polar polymers (e.g. PVAc) is the advantage regarding experimental times, because an $M(t)$ experiment detects processes within, say, 10^5 s which might need a $\sim 10^6$ s acquisition time for the classical $\epsilon(t)$ method. For PVAc near its glass transition the expected time-scale gain is a factor of 6. By measuring the voltage decay after charging the capacitor we are able to acquire $M(t)$ data in the range of $\sim 10^{-3}$–10^6 s, which roughly corresponds to dielectric $\epsilon(t)$ data in the time range $\sim 6 \times 10^{-3}$–6×10^6 s. With respect to the calorimetric glass transition, the experimental temperature range covered is $T_g^* - 13\,\text{K} \leq T \leq T_g^* + 19\,\text{K}$. As a result we find that no significant change in the distribution of relaxation times occurs in the range where the mean relaxation time is above ~10 ms.

In order to clarify the terms used below in the context of relaxation phenomena, it should be pointed out that one has to differentiate between retardation $\epsilon(t)$ for the case $\text{d}E/\text{d}t = 0$ and relaxation $M(t)$ under the condition of $\text{d}D/\text{d}t = 0$[16,19]. Typical dielectric spectroscopy thus actually refers to a retardation process, although the term 'dielectric relaxation' is generally used. Accordingly, the present experiment directly detects the relaxation function instead of a retardation process, in perfect analogy to measuring the relaxation of the shear modulus $G(t)$ instead of the retardation of the shear compliance $J(t)$ in a mechanical experiment[1,15].

EXPERIMENTAL

Sample preparation

PVAc with a viscosimetric average M_W of 14 500 and a dispersity of 3 was obtained from Wacker, FRG. The calorimetric glass transition temperature extrapolated to zero heating rate was determined by differential scanning calorimetry to be $T_g^* = 299.6\,\text{K}$. A 10% solution of PVAc in chloroform was prepared, and 10 ml of the solution was recrystallized from 1 litre petrol ether at 0°C. PVAc was then dried under vacuum for 3 days. The capacitor was prepared by melting PVAc on a 40 mm diameter gold-plated brass disc and covering the sample by a second 20 mm diameter plate. The plate separation was defined by 50 μm Teflon spacers of negligible area relative to the capacitor area.

Temperature control

The sample capacitor resided in a cryostat where cold N_2 gas emerging from a liquid nitrogen Dewar flask could be heated prior to passing the sample. The sample temperature was measured by a Pt-100 sensor mounted inside the larger brass plate of the capacitor. Each measurement was preceded by heating the sample to $T_g + 30\,\text{K}$ in order to erase residual polarizations and then equilibrating the sample at the measurement temperature for several times the average relaxation time.

Charging circuit

The aim of the charging circuit is to place a certain amount of charge onto the capacitor within a short time at $t = 0$ and without discharging the capacitor for times $t > 0$. The necessary insulation for $t > 0$ is best realized with an appropriate relay; however, relays are usually too slow for switching below 1 ms. We solved the problem by connecting a highly insulating relay in series with a fast MOSFET device, so that the high insulation of the relay is effective for $t > 10$ ms and the charging time is determined by the semiconductor, which is sufficiently fast. This is possible because the high insulation requirements are important only for times $t \gg 10$ ms. Since we are interested only in the relative decay of the field, knowledge of the amount of charge or displacement transferred to the capacitor is of minor importance. The most practical method is simply applying a preset voltage, taken from the programmable voltage source of the Keithley 6517 electrometer, to the capacitor. For the measurements presented below, a voltage of 30 V was used, although any value up to 200 V is possible with our set-up.

Detection circuit

The connection between the sample and the electrometer consisted of a coaxial air line with $C \approx 15$ pF inside the cryostat and a 50 cm low-noise triaxial cable between the cryostat and the electrometer input, with the insulation along this path exceeding $10^{15}\Omega$. We employed a Keithley Model 6517 electrometer with >200 TΩ input resistance as a voltmeter. The voltage was sampled logarithmically in time with 20 points per decade and in the range 10^{-3}–10^{6} s. For the longer times the electrometer integration time was increased to improve the signal-to-noise ratio, but with the averaging times being short compared to 1/20 of a decade. The long time limitation of the set-up can be estimated by measuring the voltage decay without the sample capacitor, so that the total cable capacity of 75 pF is discharged only thought the input resistance of the voltmeter. Such a test resulted in an exponential decay with a time constant of 1.4×10^{6} s. With the sample mounted, the minimum additional capacitance is $C_0\epsilon_\infty$, where the capacity $C_0 = \epsilon_0 A/d$ is the geometric capacity of the plates with area A and plate separation d. With $C_0 = 56$ pF and $\epsilon_\infty \approx 3.5$ for PVAc, the total capacity is at least 275 pF, which results in an upper usable limit of time range of approximately 5×10^{6} s, if the measurement is not limited by the d.c. conductivity of the sample.

Retardation measurements

The standard dielectric data $\epsilon^*(\omega)$ were measured in the frequency domain in the range 10^{-3}–10^{6} Hz using the gain-phase analysis technique with a Solartron 1260 analyser and a Novocontrol BDC-N dielectric interface. The method for temperature control was identical to that described above, but a Novocontrol Quatro system was employed in this case.

RESULTS

Relaxation

In *Figure 1* we show a series of $M(t)$ relaxation curves normalized to M_∞ for PVAc at temperatures between 291 and 323 K in steps of 2 K. A qualitative inspection of the data indicates that the curves decay from $M(t) = M_\infty$ to $M(t) = M_s$ non-exponentially with relaxation times which change by ≥ 8 decades when the temperature is varied from 291 to 323 K. The remaining decay from the slightly temperature-dependent plateau value M_s/M_∞ towards zero turns out to be an exponential process with a time constant which also shifts with temperature such that the two effects remain well separated in time. The latter effect is the signature of ohmic d.c. conductivity due to ionic impurities within the PVAc sample. Representing the contribution of the α-process by a stretched exponential or KWW decay function of the form of equation (2) leads to a satisfactory fit as shown in *Figure 1*. If we include the conductivity contribution with time constant $\sigma_{d.c.}^{-1} M_s^{-1} \epsilon_0$, the entire $M(t)/M_\infty$ curves are well represented by

$$M(t)M_\infty = (1 - M_s/M_\infty)\exp[-(t/\tau_{KWW})^{\beta_{KWW}}] + M_s/M_\infty \exp[-t\sigma_{d.c.}M_s\epsilon_0^{-1}] \quad (3)$$

where $M_s = \epsilon_s^{-1}$ and $M_\infty = \epsilon_\infty^{-1}$ denote the dielectric modulus in the limits $t \to \infty$ and $t \to 0$, respectively, regarding only the orientational polarization effects, i.e.

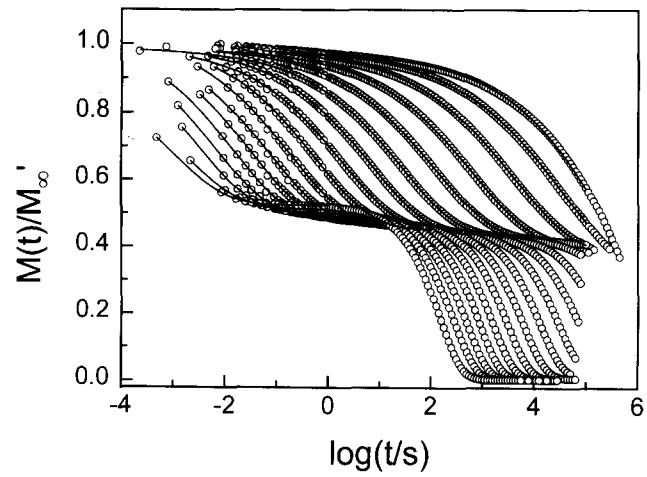

Figure 1 Experimental decay results of the dielectric modulus $M(t)$ normalized to M'_∞ for PVAc for temperatures from 291 to 323 K in steps of 2 K and in the order from slowest to fastest decay. The contributions above and below the plateau at ~0.5 reflect the α-process and d.c. conductivity, respectively. The solid lines represent KWW fits to the α-relaxation

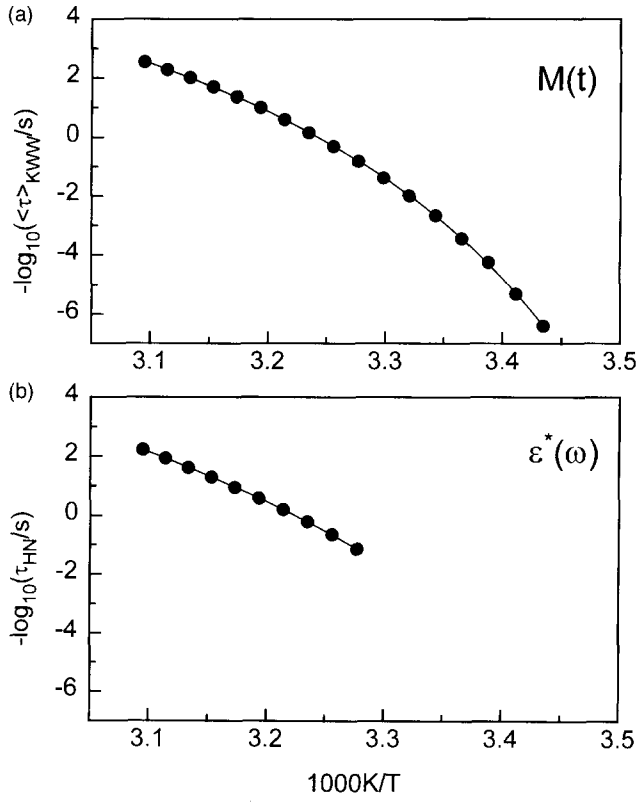

Figure 2 Activation plot, $-\log(\tau)$ *versus* $1/T$, of the temperature dependence of (a) the average dielectric relaxation time $\langle\tau\rangle_{KWW}$ derived from $M(t)$ data and (b) of the dielectric retardation time τ_{HN} derived from $\epsilon^*(\omega)$ data (HN denotes Havriliak–Negami; see text). A conversion from τ_{HN} to $\langle\tau\rangle_{KWW}$ for the $\epsilon^*(\omega)$-based data would shift the values by less than +0.1 decade only. Symbols refer to the experimental results whereas the solid lines represent VFT fits according to equation (1)

for $\sigma_{d.c.} = 0$. Since PVAc is a non-Debye dielectric with $\beta_{KWW} < 1$, we follow common practice in delineating an average relaxation time by $\langle\tau\rangle_{KWW} = \tau_{KWW}\beta_{KWW}^{-1}\Gamma(\beta_{KWW}^{-1})$ for KWW-type decays[20]. *Figure 2a* indicates the dependence of $\log_{10}\langle\tau\rangle$ for the time domain relaxation data on temperature, while the results for the KWW

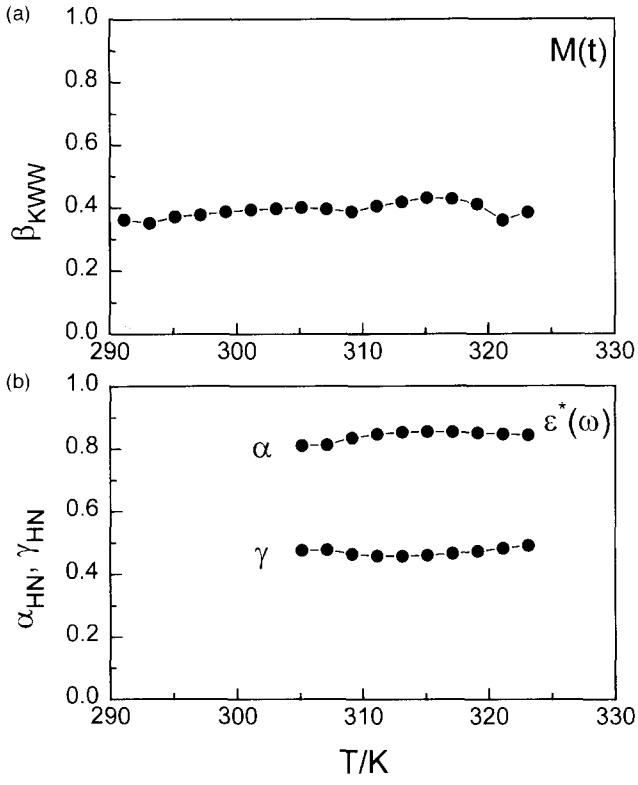

Figure 3 Temperature dependence of the shape parameters delineating the deviation from exponential or Debye-type dielectric behaviour of PVAc. (a) $\beta_{KWW}(T)$ inferred from KWW fits to the $M(t)$ relaxation data. (b) $\alpha_{HN}(T)$ and $\gamma_{HN}(T)$ inferred from HN fits to the $\epsilon^*(\omega)$ retardation data. The lines serve as guides only

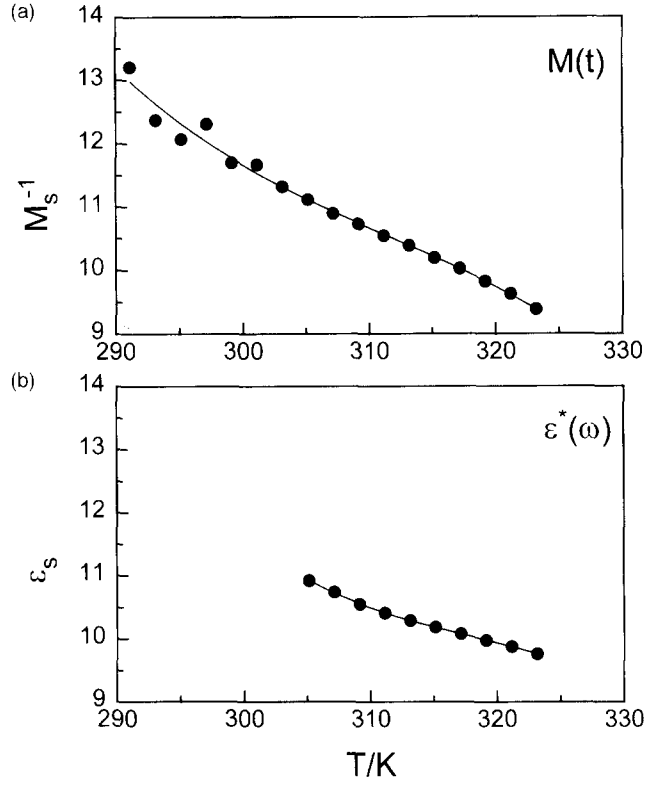

Figure 4 Temperature dependence of the static or low-frequency limit constants regarding the dielectric properties of PVAc. (a) $M_s^{-1}(T)$ on the basis of the $M(t)$ relaxation data. (b) $\epsilon_s(T)$ derived from fits to $\epsilon''(\omega)$ based on the $\epsilon^*(\omega)$ retardation data. The lines serve as guides only

dispersion parameter β_{KWW} as a function of temperature are depicted in *Figure 3a*.

From the time domain relaxation experiment as described above we can extract only the ratio M_s/M_∞ instead of the absolute values for M_s and M_∞. A straightforward solution of this problem is based on the identity $M_\infty = \epsilon_\infty^{-1}$, where ϵ_∞ can be inferred from a frequency domain relaxation experiment in terms of $\epsilon_\infty = \epsilon^*(\omega \to \infty)$. As a sufficiently good approximation, ϵ_∞ can be treated as a constant relative to the changes of ϵ_s or M_s with temperature. In practice, however, the capacity C_∞ effective for times $t \to 0$ which governs the experimentally relevant value for M_∞, M'_∞, exhibits two contributions, one from the sample capacitor, $C_0\epsilon_\infty$, and one due to the cabling of the set-up, C_c, which cannot be discriminated experimentally. The observable in the relaxation experiment is thus actually $M(t)/M'_\infty$, from which a fit according to equation (3) determines the plateau value $\rho = M_s/M'_\infty$. Knowledge of ϵ_∞ and C_c is therefore necessary in order to obtain the absolute value of M_s according to

$$M_s = \rho[\epsilon_\infty + C_c/C_0]^{-1}, \rho = M_s\, M'_\infty \qquad (4)$$

where $\rho = \rho(T)$ is the amplitude of $M(t)$ between the α-process and the conductivity decay. Employing the independently determined results for ϵ_∞ and C_c, $M_s(T)$ is calculated and plotted as $M_s^{-1}(T) = \epsilon_s(T)$ in *Figure 4a*.

Retardation

The retardation results for the identical sample but in terms of the frequency domain data $\epsilon^*(\omega)$ are displayed in *Figure 5* for temperatures ranging from 303 to 323 K, again in steps of 2 K. The experimental loss curves $\epsilon''(\omega)$ in *Figure 5* are subject to both symmetric as well as asymmetric broadening relative to the Debye case which reads $\epsilon^*(\omega) = \epsilon_\infty + (\epsilon_s - \epsilon_\infty)(1 + i\omega\tau)^{-1}$. A functional form which accounts for such deviations from a single relaxation time behaviour is the empirical dielectric function proposed by Havriliak and Negami (HN)[21]. If the appropriate term accounting for the ohmic d.c. conductivity $(-i\sigma_{d.c.}\epsilon_0^{-1}\omega^{-1})$ is added to the HN form for $\epsilon^*(\omega)$ we arrive at the fit function

$$\epsilon^*(\omega) = \epsilon_\infty + (\epsilon_s - \epsilon_\infty)[1 + (i\omega\tau_{HN})^{(\alpha_{HN})}]^{-\gamma_{HN}} - i\sigma_{d.c.}\epsilon_0^{-1}\omega^{-1} \qquad (5)$$

In equation (4) the shape parameters α_{HN}, and γ_{HN} in the limits $0 < \alpha_{HN}$, $\alpha_{HN}\gamma_{HN} \leq 1$ characterize the symmetric and asymmetric broadening, respectively, while $\alpha_{HN} = \gamma_{HN} = 1$ restores the Debye case. The HN form for $\epsilon^*(\omega) = \epsilon' - i\epsilon''$ in equation (5) yields good fits to the data in the vicinity of the peak of $\epsilon''(\omega)$, whereas the high-frequency wing displays the usual excess loss relative to the power law $\log(\epsilon'') \propto \omega^{-\alpha\gamma}$ inherent in the HN function for the range $\omega \gg \tau_{HN}^{-1}$. The parameters which are immediately obtained by fits to the retardation data $\epsilon^*(\omega)$ are the limiting dielectric constants ϵ_s and ϵ_∞, or $\Delta\epsilon = (\epsilon_s - \epsilon_\infty)$, the characteristic time constant τ_{HN}, the d.c. conductivity $\sigma_{d.c.}$, and the shape parameters α_{HN} and γ_{HN}. From τ_{HN}, α_{HN} and γ_{HN} we derive the retardation time $\tau_{max} = (\omega_{max})^{-1}$[22], where ω_{max} is given by the peak position of $\epsilon''(\omega)$. The temperature dependence of τ_{max} serving as the characteristic retardation time closely follows that of τ_{HN}, which is depicted

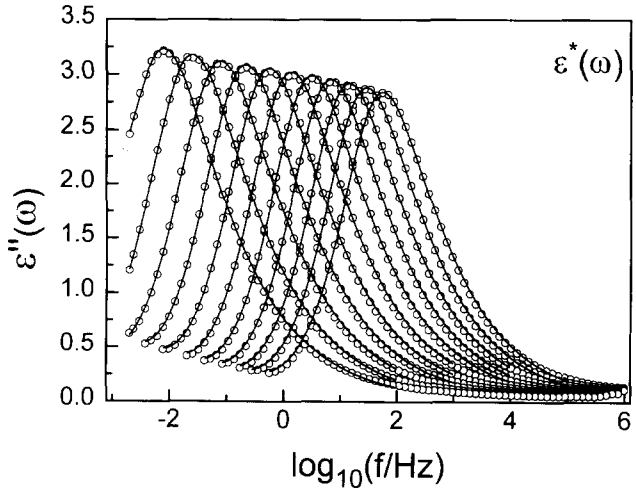

Figure 5 Experimental results for dielectric loss spectra $\epsilon''(\omega)$ versus $\log(f/\mathrm{Hz})$ of PVAc for temperatures ranging from 303 K (left curve) to 323 K (right curve) in steps of 2 K. Solid lines represent HN fits to the data

Table 1 Compilation of functions determining dielectric retardation and relaxation

	Retardation	Relaxation
Frequency domain	$\epsilon^*(\omega)$	$M^*(\omega)$
Time domain	$\epsilon(t)$	$M(t)$
Probability density of τ	$g_\epsilon(\tau)$	$g_M(\tau)$

in *Figure 2b*. The results for the shape parameters, α_{HN} and γ_{HN}, and for the static dielectric constant, ϵ_s, are compiled graphically in *Figures 3b* and *4b*, respectively.

DISCUSSION

It is common practice to display experimental dielectric retardation results $\epsilon^*(\omega)$ in terms of the modulus $M^*(\omega)$[14,23–26], for instance because a low-frequency power law of the form $\log(\epsilon'') \propto \omega^{-1}$ indicating ohmic conductivity transforms into a Debye-type loss peak for $M''(\omega)$. By virtue of the experimental conditions of a polarization-invariant dielectric displacement D_0 for times $t > 0$, the presently obtained results can be identified directly with $M(t)$, with M being the relaxation analogue of a time domain $\epsilon(t)$ retardation experiment. Regarding the application to the extremely long relaxation times of PVAc we exploit the fact that for a given dielectric sample displaying orientational polarizability the quantity $M(t)$ decays faster than its relaxation counterpart $\epsilon(t)$. The extent of the relative acceleration of $M(t)$ grows with increasing polarity or relaxation strength $\Delta\epsilon$. In the opposite situation of unpolar systems with $\Delta\epsilon \approx 0$, one has $M(t) \propto \epsilon(t)$, and the discrepancy between relaxation and retardation vanishes.

In order to demonstrate the basic equivalence of the information contained in the different quantities, a summary of the necessary transformations among the functions compiled in *Table 1* appears in order. Within one group, $x^*(\omega)$, $x(t)$ and $g_x(\tau)$, where x stands for ϵ or M, the relations between $x^*(\omega)$ and $x(t)$ are given by Fourier transforms in either direction, and $x(t)$ emerges from $g_x(\tau)$ by means of a Laplace transform, which for $x = M$ reads

$$M(t) = M_s + (M_\infty - M_s)\int_0^\infty g_M(\tau)\mathrm{e}^{-t/\tau}\mathrm{d}\tau \qquad (6)$$

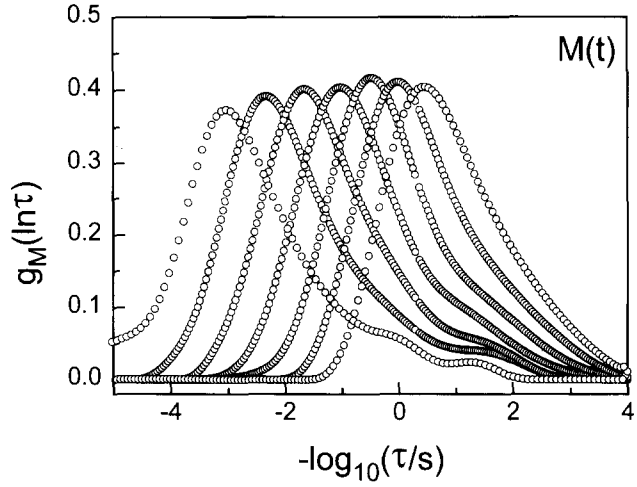

Figure 6 Numerically determined probability density of the logarithm of relaxation times $g_M(\ln\tau) = \tau g_M(\tau)$, calculated on the basis of experimental $M(t)$ relaxation data, with the relation between $g_M(\tau)$ and $M(t)$ as stated in equation (6). The results are shown for the intermediate temperatures, 299–307 K, in steps of 2 K, where the transformation yields reliable $g_M(\tau)$ curves

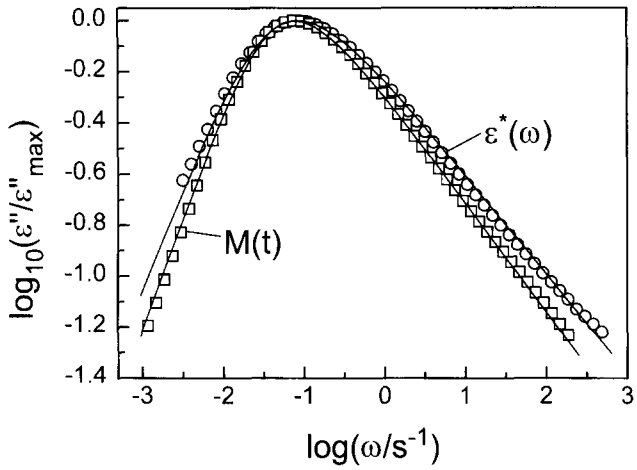

Figure 7 Comparison of two dielectric loss spectra obtained for PVAc at $T = 307$ K and plotted as $\epsilon''(\omega)/\epsilon''_{max}$ *versus* $\log(\omega/\mathrm{s}^{-1})$. The curve marked '$\epsilon^*(\omega)$' is a direct result of a frequency domain dielectric retardation measurement. The curve marked '$M(t)$' represents time domain $M(t)$ relaxation data, but transformed according to the scheme $M(t) \rightarrow g_M(\ln\tau) \rightarrow M^*(\omega) \rightarrow \epsilon^*(\omega)$. Solid lines represent HN fits according to equation (5)

Because either $x^*(\omega)$ or $x(t)$ is the measured quantity, one is often more interested in obtaining $g_x(\tau)$ from one of the two functions. For real $x^*(\omega)$ or $x(t)$ data, i.e. curves subject to random noise, the determination of a non-negative $g_x(\tau)$ has an infinite number of 'acceptable' solutions, i.e. the problem is ill-defined[27]. A more realistic solution of the problem is finding the smoothest representation for $g_x(\tau)$ but with only little excess deviation relative to the mathematically best fit. With appropriate regularization techniques and for sufficiently noise-free data such a probability density of relaxation or retardation times can be obtained numerically with stable and well-tested algorithms[28,29]. Once $g_x(\tau)$ is known to a certain degree of accuracy, the two functions $x^*(\omega)$ or $x(t)$ can be recovered easily.

The relation between retardation and relaxation is trivial only for the frequency domain representation, where $\epsilon^*(\omega) = [M^*(\omega)]^{-1}$, and the remaining relations

$\epsilon(t) \leftrightarrow M(t)$ and $g_\epsilon(\tau) \leftrightarrow g_M(\tau)$ involve integral equations which are difficult to handle numerically[30,31]. For a comparison of our $M(t)$ and $\epsilon^*(\omega)$ results, we therefore select the route of finding $g_M(\tau)$ using the numerical procedure realized by Schäfer *et al.*[28]. Based on the result of $g_M(\tau)$ we obtain $M^*(\omega)$ via a Stieltjes transform. Inverting to the form $[M^*(\omega)]^{-1}$ then yields a representation of the relaxation data which is expected to be equal to the independently measured $\epsilon^*(\omega)$. For a reliable numerical analysis which transforms $M(t)$ to $g_M(\tau)$ it is essential that the entire decay has been recorded, i.e. this procedure is applicable only to intermediate temperatures, where all decay contributions are accurately resolved in the range 10^{-2}–10^5 s. Relaxation time distribution results obtained along the above lines are shown as $g_M(\ln\tau) = \tau g_M(\tau)$ in *Figure 6* for several temperatures where the relaxation times τ cover a range $10^{-1}\,\text{s} \leq \tau \leq 10^4$ s. In accord with the retardation spectra $\epsilon^*(\omega)$ for PVAc the $g_M(\ln\tau)$ curves feature both symmetric and asymmetric broadening as well as an excess contribution in the outer high-frequency wing. Additionally, the similarity of the relaxation time distributions for various temperatures demonstrates the reliability of the numerically non-trivial $M(t) \rightarrow g_M(\ln\tau)$ transformation and the absence of any significant changes near the calorimetric T_g^*.

The achieved knowledge of $g_M(\ln\tau)$ now facilitates calculation of the complex modulus $M^*(\omega)$ and thus the dielectric function $\epsilon^*(\omega)$ as derived from experimental $M(t)$ data. A representative comparison of the $M(t)$ data transformed to $\epsilon^*(\omega)$ with the directly measured $\epsilon^*(\omega)$ results is shown in *Figure 7* in terms of the normalized frequency-dependent loss $\epsilon''(\omega)/\epsilon''_{\max}$. In view of the necessary transformation involved, $M(t) \rightarrow g_M(\ln\tau) \rightarrow M^*(\omega) \rightarrow \epsilon^*(\omega)$, we understand the similarity of these loss spectra as a strong indication for our field decay experiment under the condition $\mathrm{d}D/\mathrm{d}t = 0$ measuring the dielectric modulus $M(t)$ as expected. Further support for this notion derives from the almost identical results for $d\langle\tau\rangle_{\mathrm{KWW}}/\mathrm{d}T$ and $\mathrm{d}\tau_{\mathrm{HN}}/\mathrm{d}T$ in *Figure 2*, for $\epsilon_s(T)$ and $M_s^{-1}(T)$ in *Figure 4*, and from the approximately temperature-independent shape parameters β_{KWW} and the respective quantities α_{HN} and γ_{HN} in *Figure 3*.

The compatibility of $\epsilon^*(\omega)$ and $M(t)$ as demonstrated above justifies employing the $M(t)$ relaxation data for analysing the dielectric behaviour in the ultra-slow time regime. With respect to the average relaxation times $\langle\tau\rangle_{\mathrm{KWW}}$ we have gained access to values ranging from 3×10^{-3} to 2×10^6 s. In terms of the average retardation times $\langle\tau\rangle$ usually inferred from $\epsilon^*(\omega)$ or $\epsilon(t)$ experiments, this range corresponds to values between 1.5×10^{-2} and 1×10^7 s (10^7 s = 116 days). The coincidence between the α-process contribution to $M(t)$ data and the KWW fits together with the observation of a nearly temperature-independent shape parameter β_{KWW} over the entire experimental temperature range implies that the shape of the relaxation time distribution remains basically unchanged. Relative to the time-scale τ_g at the 'glass transition' temperature T_g^* where $\tau_g = \langle\tau_\epsilon\rangle_g = 100$ s, we therefore observe the absence of significant changes in the shape of $g_M(\ln\tau)$ in the range $10^{-3}\,\tau_g \leq \langle\tau_\epsilon\rangle \leq 10^5\,\tau_g$. That this conclusion relates to equilibrium conditions even for very low temperatures is demonstrated by the mean relaxation times following a single VFT dependence and by the steady curvature of the static modulus constant M_s *versus* T, both within the entire temperature range. In the less favourable case where a constant $g_M(\ln\tau)$ would have resulted from identical effective temperatures below T_g due to insufficient equilibration, the concomitant $\langle\tau\rangle(T)$ data would have departed strongly from the VFT behaviour at $T \leq T_g$. Therefore, the present experimental conditions have shifted the kinetic T_g of PVAc to lower temperatures by ~10 K, if a kinetic T_g is understood as the temperature at which the material no longer equilibrates on the time-scale of the experiment. In conclusion, the experiments clearly indicate that no effects other than purely kinetic occur when slowing down the molecular motion by lowering the temperature such that time-scales of up to 10^7 s become relevant.

The above results contrast with a former study on PVAc by Nozaki and Mashimo[11], who claimed to observe a drastic alteration in the symmetry of the retardation time distribution near the calorimetric glass transition at $T_g^* = 31$°C. The polymer used in their study displays a different molecular weight relative to our material, so that we refrain from a detailed quantitative comparison. An ambiguity in the former work is believed to be the change from the frequency domain $\epsilon^*(\omega)$ technique to the time domain $\epsilon(t)$ instrumentation exactly at $T_g^* = 31$°C in conjunction with only approximate numerical procedures used for the $\epsilon(t) \rightarrow \epsilon^*(\omega)$ transformation. Secondly, the $\alpha_{\mathrm{HN}}(T)$ and $\gamma_{\mathrm{HN}}(T)$ data reported in the former study indicate systematic changes of the two shape parameters ($\Delta\alpha_{\mathrm{HN}} = -0.08$, $\Delta\gamma_{\mathrm{HN}} = +0.05$) below ~45°C within the frequency domain data set. However, an analysis of such a simultaneous alteration of both α_{HN} and γ_{HN} shows that the resulting dielectric loss curves $\epsilon''(\omega)$ are affected only to a subtle extent, i.e. the effects of a decreasing α_{HN} and an increasing γ_{HN} almost cancel each other with respect to the shape of $\epsilon''(\omega)$. Relative to the approach used by Nozaki and Mashimo, we believe that a single measurement technique used below and above T_g^*, reduction of the shape analysis to only one parameter β_{KWW}, and unbiased numerical transforms leads to more conclusive results regarding the trend of the relaxation time distribution upon changing the temperature towards extremely long relaxation time-scales.

As discussed above, we have measured also the usual $\epsilon^*(\omega)$ retardation data in addition to the $M(t)$ relaxation data for the identical sample. The measured $\epsilon^*(\omega)$ results are not evaluated in quantitative detail, but used here only to demonstrate the equivalence of the dielectric properties of PVAc inferred from $M(t)$ and $\epsilon^*(\omega)$ experiments. A more critical comparison of the two techniques reveals minor but systematic differences which are close to the experimental resolution: (i) $M_s^{-1}(T)$ decreases slightly stronger with T as does the equivalent $\epsilon_s(T)$ curve, (ii) the loss profile $\epsilon''(\omega)$ derived from $M(t)$ data is somewhat narrower relative to the direct $\epsilon^*(\omega)$ result, and (iii) the high-frequency wing of $\epsilon''(\omega)$ derived from $M(t)$ data is not subject to the typical departure from an HN-type power law. At present, the experimental findings only point tentatively towards a subtle but physically significant difference between $M^*(\omega)$ and $\epsilon^*(\omega)$ beyond the relation $M^*(\omega) = 1/\epsilon^*(\omega)$, which certainly holds for simple continuum dielectrics.

In summary, we have measured the dielectric orientational relaxation $M(t)$ for the first time directly by monitoring $E(t)$ at constant displacement D_0. Taking advantage of the fact the $M(t)$ decays faster than $\epsilon(t)$ for

polar materials such as PVAc, we are able to access average retardation times in the range 1.5×10^{-2}–1×10^{7} s with a single experimental technique. A numerical comparison to $\epsilon^*(\omega)$ retardation data confirms the expected $\epsilon^*(\omega) \leftrightarrow M(t)$ relation. As a result, we find that the relaxation time distribution function is practically constant for temperatures ranging from well above T_g^* to well below T_g^*, where the retardation time τ is five orders of magnitude larger than τ_g defined via $\tau_g = \tau(T = T_g^*) = 100$ s. This observation strongly argues in favour of the glass transition being a purely kinetic effect based on the competition between relaxation or retardation time-scale and the experimental time window. In other words, if the experimental time limit is sufficiently extended, PVAc still displays liquid-like behaviour up to time-scales of the segmental motion of 116 days.

ACKNOWLEDGEMENTS

We thank U. Albrecht and H. Schäfer for valuable assistance in the numerical determination of the distribution functions. Financial support by the Fonds der Chemischen Industrie is gratefully acknowledged.

REFERENCES

1 McCrum, N. G., Read, B. E. and Williams, G. 'Anelastic and Dielectric Effects in Polymeric Solids', Dover, New York, 1991
2 Jäckle, J. *Rep. Prog. Phys.* 1986, **49,** 171
3 Richert, R. and Blumen, A. (Eds) 'Disorder Effects on Relaxational Processes', Springer-Verlag, Berlin, 1994
4 Kovacs, A. J. *J. Polym. Sci.* 1958, **30,** 131
5 Kauzmann, W. *Chem. Rev.* 1948, **43,** 219
6 Vogel, H. *Phys. Z.* 1921, **22,** 645
7 Fulcher, G. S. *J. Am. Ceram. Soc.* 1923, **8,** 339
8 Kohlrausch, R. *Pogg. Ann. Phys.* 1854, **91,** 179
9 Williams, G. and Watt, D. C. *Trans. Faraday Soc.* 1970, **66,** 80
10 Ferry, J. D. 'Viscoelastic Properties of Polymers', 3rd edn, Wiley, New York, 1980
11 Nozaki, R. and Mashimo, S. *J. Chem. Phys.* 1987, **87,** 2271
12 Scaife, B. K. P. 'Principles of Dielectrics', Clarendon Press, Oxford, 1989
13 Mopsik, F. I. *Rev. Sci. Instrum.* 1984, **55,** 79
14 Schiener, B. and Böhmer, R. *J. Non-Cryst. Solids* 1995, **182,** 180
15 Donth, E. 'Relaxation and Thermodynamics in Polymers', Akademie Verlag, Berlin, 1992
16 Fröhlich, H. 'Theory of Dielectrics', Clarendon Press, Oxford, 1958
17 Richert, R. and Wagner, H. *J. Phys. Chem.* 1995, **99,** 10948
18 Kivelson, D. and Friedman, H. *J. Phys. Chem.* 1989, **93,** 7026
19 Friedman, H. *J. Chem. Soc., Faraday Trans. 2* 1983, **79,** 1465
20 Lindsey, C. P. and Patterson, G. D. *J. Chem. Phys.* 1980, **73,** 3348
21 Havriliak, S. and Negami, S. *J. Polym. Sci., Polym. Symp.* 1966, **14,** 89
22 Stickel, F., Fischer, E. W. and Richert, R. *J. Chem. Phys.* 1995, **102,** 6251
23 Elliott, S. R. *J. Non-Cryst. Solids* 1994, **170,** 97
24 Floriano, M. A. and Angell, C. A. *J. Chem. Phys.* 1989, **91,** 2537
25 Tombari, E. and Johari, G. P. *J. Chem. Phys.* 1992, **97,** 6677
26 Macedo, P. B., Moynihan, C. T. and Bose, R. *Phys. Chem. Glasses* 1972, **13,** 171
27 Landl, G., Langthaler, T., Engl, H. W. and Kauffman, H. F. *J. Comp. Phys.* 1991, **95,** 1
28 Schäfer, H., Albrecht, U. and Richert, R. *Chem. Phys.* 1994, **182,** 53
29 Albrecht, U., Schäfer, H. and Richert, R. *Chem. Phys.* 1994, **182,** 61
30 Gross, B. *Kollaid Z.* 1953, **131,** 168
31 Gross, B. *Kollaid Z.* 1953, **134,** 65